Free Radical Research, November 2006; 40(11): 1173–1181

informa
healthcare

Proteomic analysis for protein carbonyl as an indicator of oxidative damage in senescence-accelerated mice

HIROMI NABESHI[1], SHINJI OIKAWA[1], SUMIKO INOUE[2], KOHSUKE NISHINO[3] & SHOSUKE KAWANISHI[1]

[1]*Department of Environmental and Molecular Medicine, Mie University Graduate School of Medicine, Mie, Japan,* [2]*Department of Health Environmental Sciences, Kyoto University School of Public Health, Kyoto, Japan, and* [3]*Department of Food Science and Nutrition, Faculty of Human Life and Science, Doshisha Women's College, Kyoto, Japan*

Accepted by Professor E. Niki

(Received 5 October 2005; in revised form 5 December 2005)

Abstract

The senescence-accelerated prone mouse strain 8 (SAMP8) exhibits a remarkable age-accelerated deterioration in learning and memory. In this study, we identified carbonyl modification, a marker of protein oxidation, in liver and brain of SAMP8 from peptide mass fingerprints using MALDI-TOF mass spectrometry in combination with LC-MS/MS analysis. Carbonyl modification of Cu,Zn-superoxide dismutase (Cu,Zn-SOD) in liver at 3 month and hippocampal cholinergic neurostimulating peptide precursor protein (HCNP-pp) in brain at 9 month were higher in SAMP8 compared with control SAMR1. We demonstrated carbonyl modification of purified Cu,Zn-SOD increased by the reaction with H_2O_2. Therefore, progressive accumulation of oxidative damage to Cu,Zn-SOD, may cause dysfunction of defense systems against oxidative stress in SAMP8 with a higher oxidative states, leading to acceleration of aging. Furthermore, carbonyl modification of HCNP-pp may be involved in pathophysiological alterations associated with deterioration in the learning and memory in the brain seen in SAMP8.

Keywords: *Senescence-accelerated mouse, proteomics, aging, carbonyl protein, reactive oxygen species*

Abbreviations: *SAMP, senescence-accelerated prone mouse; SAMR, senescence-accelerated resistant mouse; SBP, selenium binding protein; GRP78/Bip, 78 kDa glucose-regulated protein; PDI, protein disulfide isomerase; MAT, methionine adenosyltransferase; MUP, major urinary protein; HCNP-pp, hippocampal cholinergic neurostimulating peptide precursor protein; AD, Alzheimer's disease; DNP, 2,4-dinitrophenylhydrazone; DNPH, 2,4-dinitorophenylhydrazine*

Introduction

The senescence-accelerated prone mouse (SAMP) strain has been widely used as an animal model of senescence acceleration and various age-associated disorders observed in humans [1,2]. SAMP strain exhibits a short life span in addition to early signs of various indices of aging [3–5] and shows a higher oxidative status in various organs such as brain, liver, heart, eye and so forth [6]. Among the many SAM substrains, SAMP8 exhibits remarkable deficits in learning and memory as an age-related disorder at earlier stage of their life span than control SAMR1 [7]. As the age-related morphological changes in SAMP8 brain, massive occurrences of PAS-positive granular structures (PGS) in the hippocampus and spongiform degeneration of the reticular formation of the brain

Correspondence: S. Kawanishi, Department of Environmental and Molecular Medicine, Mie University Graduate School of Medicine, Mie, Japan. E-mail: kawanisi@doc.medic.mie-u.ac.jp

Present address: S. Kawanishi, Faculty of Health Science, Suzuka University of Medical Science, 1001-1 Kishioka, Suzuka, Mie 510-0293, Japan

ISSN 1071-5762 print/ISSN 1029-2470 online © 2006 Informa UK Ltd.
DOI: 10.1080/10715760600847580

stem were observed [8]. Although various studies have assessed systematically and dynamically these age-related pathologies in the SAMP8 strain, the major molecular factors responsible for accelerated senescence have not been elucidated [9].

Carbonylated protein is a marker of protein oxidation and implicates in aging and age-related diseases deeply. Oxidative damage to proteins can lead to loss in specific protein function [10,11]. Age-related increases in carbonyl modification of proteins were observed in various tissues of several animals [11]. Interestingly, accumulation of protein carbonyls is associated with a number of age-related diseases, particularly Alzheimer's disease, progeria and Werner's syndrome [11].

Using proteomics tools, we compared oxidative damage to proteins and the alteration of protein expression in liver in two age groups (3-month old and 9-month old) of SAMP8 and SAMR1. Identification of specific carbonyl modified protein might be available for establishing a relationship between oxidative damage to proteins and aging [12]. In this study, we identified specific carbonyl modified protein in liver and brain tissues between two SAM strains (SAMR1 and SAMP8) by two-dimensional gel electrophoresis (2DE) with immunochemical detection of protein carbonyls (2D Oxyblot) and peptide mass fingerprinting (2D-gel fingerprinting). The identification of specific carbonyl modified protein was validated by liquid chromatography combined with tandem mass spectrometry (LC-MS/MS).

Experimental

Sample preparation

The mice used in this study were male SAMR1 and SAMP8 of 3-month old and 9-month old. Liver and brain tissues were excised immediately under ether anesthesia and stored at −80°C until use. About 0.5 mg of frozen livers and whole brains from three mice were homogenized with 9 volumes and 4 volumes of homogenizing buffer containing phosphate buffered saline (PBS), 0.1% TritonX-100 and 1 mM EDTA, respectively. Both samples were centrifuged at 15,000*g* for 10 min at 4°C. The supernatant containing microsomes and cytoplasm was stored at −80°C until use after the protein level was measured using BCA assay (PIERCE).

Quantitative analysis of protein carbonyl level in liver and brain

Quantitative analysis of protein carbonyl level was performed as described previously [13]. A volume of samples containing 0.1 mg of protein were mixed with equal volume of 20% trichloroacetic acid (TCA) (final concentration of 10%) and centrifuged at 15,000*g* for 3 min at 4°C. The pellets were incubated with 10 mM 2,4-dinitrophenylhydrazine in 2 M HCl for 60 min at 37°C. Proteins were then precipitated by addition of ice-cold TCA to obtain a final concentration of 10% TCA. The pellets were washed with 1 ml of ethanol–ethyl acetate (1:1) to remove free reagent and solubilized with 1 ml of 6 M guanidine HCl, 20 mM potassium phosphate (pH 2.3) with vortexing for 15 min at 37°C. Calculate the carbonyl content from the maximum absorbance (362 nm) using a molar absorption coefficient of 22,000 M^{-1} cm^{-1}.

Two-dimensional gel electrophoresis (2DE) and image analysis

A volume of the protein samples containing 500 μg of protein were mixed with equal volume of 20% TCA (final concentration of 10%) and centrifuged at 15,000*g* for 3 min at 4°C. The pellets were immediately washed with ethanol and solubilized with rehydration solution containing 8 M urea, 2% TritonX-100, 0.5% IPG buffer (pH 4–7, Amersham Bioscience), 0.28% dithiothreitol (DTT) and a trace of bromophenol blue (BPB). Solubilized samples were applied to Immobiline Drystrips (18 cm, pH 4–7, Amersham Bioscience). The strips were then loaded onto an IPGphor (Amersham Bioscience) and covered with layer of Drystrip cover fluid (Amersham Bioscience). The strips were rehydrated for 12 h at 20°C and then isoelectric focusing (IEF) was carried out for a total of 51,500 Vh (gradient mode). After IEF, the strips were equilibrated for 2 × 15 min under gentle shaking in equilibration buffer (50 mM Tris/HCl pH 8.8, 6 M urea, 30% glycerol, 2% SDS, 1% DTT and a trace of BPB). Iodoacetamide (2.5%) was added to the second equilibration buffer instead of DTT. The strips were transferred for second dimension onto vertical gradient slab gels (PAG large "Daiichi" 2D-10/20 (0.9), Daiichichem) and overlaid with 1% low melting agarose in standard SDS running buffer. Standard SDS-PAGE was performed at room temperature using 50 mA/gel until the tracking dye (BPB) reached the bottom of the gel. Gels were stained with Coomassie Brilliant Blue R-350 (CBB, Amersham Bioscience). The stained gels were scanned using a Personal Densitometer SI (amersham pharmacia biotech) and analyzed with Image Master Elite v 4.01 (Amersham Bioscience). Image analysis included the following steps: spot detection, spot editing, background subtraction, spot matching and spot intensity normalization. Expression levels were determined from the relative spot intensity of each protein versus other non-relative spots on a CBB stained gel and Oxyblot membrane. For proteome analysis, three sheets of 2D gels per group were prepared. We selected the spots of 1.5-fold and over alteration in each comparison and carried out in gel digestion.

In gel digestion and mass spectrometric analysis

CBB 2DE spots were excised from gels with scalpel. The gel pieces were destained with 30% acetonitrile in 25 mM ammonium bicarbonate at room temperature. Destained gel pieces were dehydrated with 100% acetonitrile and dried in a SpeedVac (Savant). The dried gel pieces were incubated in 15 μl of 11 μg/ml trypsin (Promega) solution for 24 h at 37°C. The resultant peptide mixtures were extracted twice with 50 μl of 5% trifluoroacetic acid (TFA)/50% acetonitrile. The extracted peptides were concentrated in a SpeedVac. Mass analysis of peptide mixtures was performed using a Voyager B-RP (PerSeptive Biosystems) MALDI-TOF mass spectrometer operating in positive-ion reflector mode. Peptide mixture was deposited onto the MALDI target closely followed by matrix solution containing 50% α-cyano-4-hydroxycinnamic acid (Aldrich) in 0.5% trifluoroacetic acid/50% acetonitrile and air-dried. TOF spectra were collected over the mass range of 500–4000 Da and calibrated using Sequazyme Peptide Mass Standard Kit (Applied Biosystems). If the mass spectra were of poor quality, the peptide extracts were concentrated and desalted using in-tip reversed-phase resin (Zip tip C18; Millipore) and the MALDI MS analysis repeated. Protein database searching was performed with MS-fit program using monoisotopic peaks. The resulting peptide masses were identified by searches of a rodent subset of the SWISS-PROT, NCBInr and Owl databases.

Detection of carbonyl modified proteins (2D Oxyblot analysis)

Carbonylated proteins were labeled by derivatization of carbonyl group with 2,4-dinitrophenylhydrazone (DNP) by reaction with 2,4-dinitrophenylhydrazine (DNPH) and then detected, using an antibody specific to the DNP moiety (Oxyblot Protein Oxidation Detection Kit, CHEMICON). Proteins precipitated with 10% TCA were suspended and incubated in DNPH solution for 60 min at room temperature. The resulting protein hydrazones were pelleted in a centrifuge at 15,000*g* for 3 min at 4°C. The pellets were washed twice with 1 ml of ethanol and then once with acetone. The final precipitates were dissolved in rehydration solution and carried out 2DE as described above. Following 2DE, standard electrotransblotting to PVDF membrane (Immobilon-P, MILLIPORE) was carried out by Horizblot semidry electrotransblotting unit (ATTO) for 30 min at 2 mA/cm^2. After electrotransblotting, the membrane was immnostained using rabbit anti-DNP antibody as primary antibody, goat anti-rabbit IgG (HRP-conjugated) as second antibody (Oxyblot Protein Oxidation Detection Kit, CHEMICON) and chemiluminescent reagent (BM Chemiluminescence Blotting Substrate, Roche). Autoradiograms were obtained by exposing an X-ray film to the membrane for various time intervals. In order to identify the proteins detected by 2D-Oxyblot analysis, we analyzed the corresponding protein that was stained with CBB on the 2D-gel by MALDI-TOF mass spectrometer.

LC-MS/MS analysis

Peptides generated from tryptic digestion were loaded at high flow rate into a reverse-phase trapping column (0.30 mm i.d., C18PM, LC Packings) and eluted through a reverse-phase capillary nanocolumn (75 μm i.d. × 15 cm, C18 PepMap100, 3 μm, 100 Å, LC Packings) directly into the nano-electrospray ion source of a quadrupole time-of-flight mass spectrometer (Q-TOF Ultima Global, Micromass). Mass data collected during an LC-MS/MS analysis were processed and converted into a pkl file using the Masslynx^{TM} software (Micromass) to be submitted to the search software Mascot (Matrix Science). Peptide identifications were obtained by comparison of experimental data to the NCBInr database.

Detection of carbonyl modification of Cu,Zn-SOD in the presence of H_2O_2

The reaction mixtures that contained 5 μM Cu,Zn-superoxide dismutase ((Cu,Zn-SOD), Human, Recombinant, *E. coli*, CALBIOCHEM), and 1.0 mM H_2O_2 in 500 μl of 23.5 mM $NaHCO_3/CO_2$ buffer (pH 7.6) were incubated at 37°C for 60 min. After incubation, 500 μl of 20% TCA was added to the reaction mixtures and centrifuged at 15,000*g* at 4°C for 5 min. Protein pellets were suspended and incubated in DNPH solution for 60 min at room temperature. The pellets were washed with ethanol and then acetone. The final precipitates were dissolved in 10 μl of 2 × SDS sample lording buffer (50 mM Tris (pH 6.8), 2% SDS, 5% mercapto ethanol, 10% glycerol, 0.02% BPB) and carried out SDS-PAGE using a gradient of 15–25% polyacrylamide gel (PAG Mini "Daiichi" 15/25 13 well, Daiichichem). As an internal standard, the samples containing 5 μM Cu,Zn-SOD in 2 × SDS sample lording buffer were analyzed by SDS-PAGE and electrotransblotting. Then, immunostaing were carried out using sheep antisuperoxide dismutase (Cu/Zn Enzyme) antibody as primary antibody (CHALBIOCHEM), rabbit anti-sheep IgG (HRP-conjugated) as second antibody (Santa Cruz Biotechnology, Inc.). Following SDS-PAGE, electrotransblotting and immunostaing were carried out as described above.

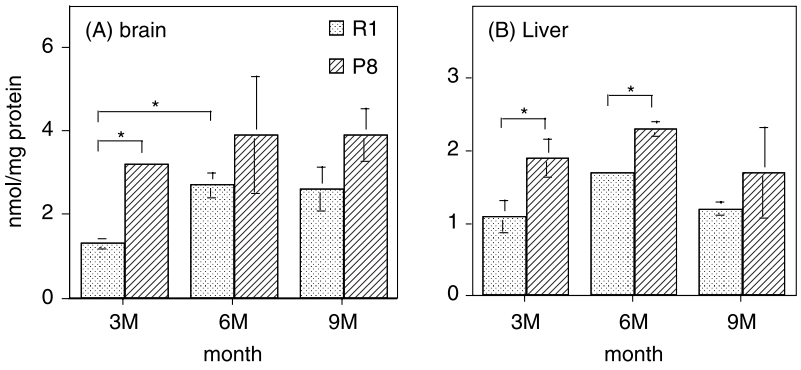

Figure 1. Comparison between protein carbonyl contents in brains (A) and livers (B) of male SAMP8 and SAMR1 during aging. Values represent means ± SD of 3 mice. Asterisk is given where a significant difference between two columns is observed ($p < 0.01$).

Results

The level of protein carbonyl in brain and liver

The level of protein carbonyl in brain of SAMP8 was significantly higher than those of SAMR1 already at 3 months of age (Figure 1(A)). Protein carbonyl level in liver of SAMP8 was also higher than that of SAMR1 (Figure 1(B)). The increase of protein carbonyl contents with age was not significant either in the brain or in the liver of SAMP8.

The carbonyl modified protein identification

Carbonyl modified proteins from the liver at 3 month (Figure 2) and the brain (Figure 3) at 9 month were determined by 2D-Oxyblot analysis. We focused on proteins that changed at least >1.5-fold between SAMP8 and SAMR1. A total of 35 carbonylated protein spots were detected in liver (Figure 2). The carbonylated proteins with down-regulation in liver of SAMP8 compared with SAMR1 were 3 spots (Figure 2(A)) and the proteins with up-regulation were 11 spots (Figure 2(B)). Spot number c14 with higher carbonyl modification in SAMP8 liver was identified as Cu,Zn-SOD by peptide mass fingerprinting using MALDI-TOF mass spectrometer. Furthermore, spots of higher carbonyl levels c4, c6, c7, c9 and c12 were also identified as 78 kDa glucose-regulated protein (GRP78/Bip) which is a molecular chaperone induced by ER stress, serum albumin, protein disulfide isomerase ER-60 (PDI), selenium binding liver protein (SBP) and major urinary protein (MUP), respectively. However, there was no increase in non-carbonylated protein expression levels of Cu,Zu-SOD, GRP/Bip, serum albumin, PDI and SBP in SAMP8.

A total of 24 carbonylated protein spots were detected in the brain (Figure 3). The carbonylated proteins with up-regulation in the brain of SAMP8 compared with SAMR1 were 3 spots (Figure 3(B))

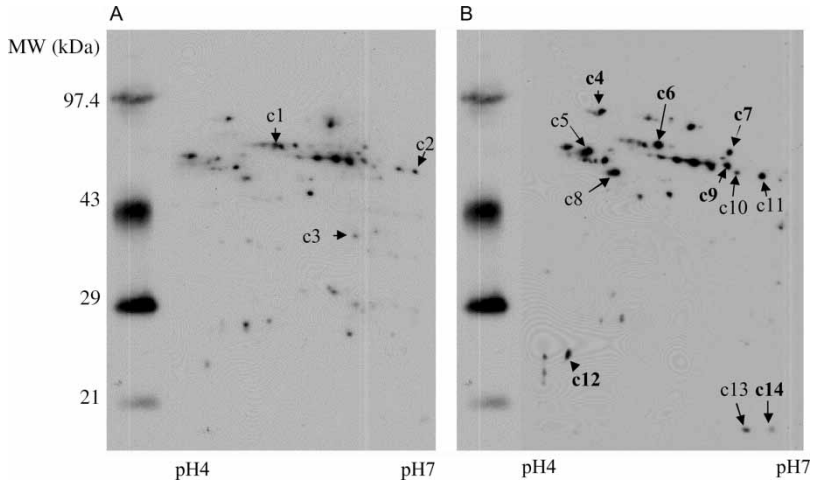

Figure 2. 2D-Oxyblot analysis of carbonylated proteins from liver of SAMR1 and SAMP8. Solublized liver proteins from SAMR1 (A) and SAMP8 (B) were derivatized with DNP. Following 2DE and transfer to PVDF, the derivatized proteins were detected using a DNP-specific antibody. A total of 35 carbonylated protein spots were detected in liver. Arrows show (A) lower (< −1.5-fold) and (B) higher (>1.5-fold) carbonyl modification of proteins in SAMP8 compared with SAMR1.

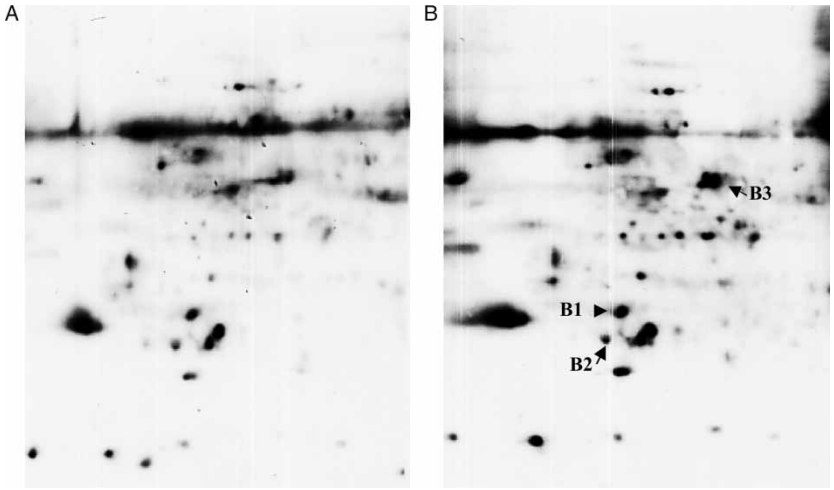

Figure 3. 2D-Oxyblot analysis of carbonylated proteins from brain of SAMR1 and SAMP8. A shows carbonylated proteins, which were detected in SAMR1; B shows that in SAMP8 and arrows show higher (>1.5-fold) than in SAMR1 with reproducibility.

with reproducibility. Spot number B2 with increased carbonyl modification in SAMP8 brain was identified as hippocampal cholinergic neurostimulating peptide precursor protein (HCNP-pp).

In order to confirm the results of MALDI-MS analysis, we performed LC-MS/MS analysis. The MS/MS spectrum of the precursor ion mass at *m/z* 684.32 derived from a tryptic peptide of spot c14 is shown in Figure 4. The observed sequence was identified to be VISLSGEHSIIGR, which completely matched Cu,Zn-SOD fragment (aa 103–115). This result supports that spot c14 corresponds to Cu,Zn-SOD, as well as MALDI-MS analysis. In the same way, the spot number c4, c6, c7, c9, c12 and B2 were also identified as GRP78/Bip, serum albumin, PDI, SBP and HCNP-pp, respectively (data not shown).

Carbonyl modification of purified Cu,Zn-SOD induced by H_2O_2

To elucidate the mechanism of carbonylation of Cu,Zn-SOD, we examined carbonyl modification of purified Cu,Zn-SOD induced by H_2O_2. No carbonyl modification of Cu,Zn-SOD was detected without H_2O_2 treatment (Figure 5, upper panel, lane 1). Carbonyl modification of Cu,Zn-SOD treated with

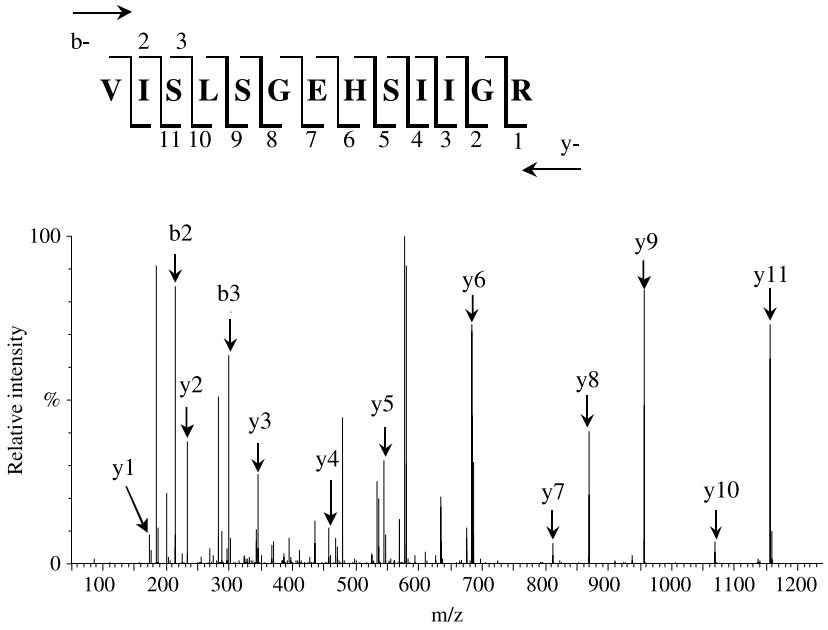

Figure 4. LC-MS/MS spectrum of an in-gel tryptic digest obtained from spot c14. The doubly charged precursor ion at *m/z* 684.32 corresponds to the peptide with the sequence VISLSGEHSIIGR from Cu,Zn-SOD. Annotations indicate detectable singly charged b-ion species (b2, b3) and y-ion species (y1–y11) that generated by collision-induced dissociation.

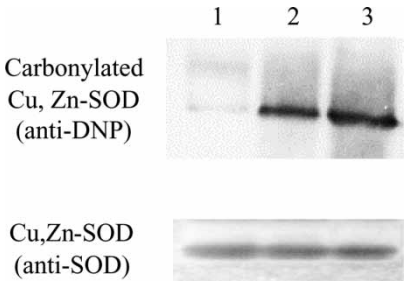

Figure 5. Carbonyl modification of purified Cu,Zn-SOD induced by H_2O_2. Equal amounts of purified Cu,Zn-SOD (5 μM = 58.8 μg) were incubated with several concentration of H_2O_2 in 23.5 mM $NaHCO_3/CO_2$ at 37°C for 60 min. After the incubation, Cu,Zn-SOD was incubated in DNPH solution and then, separated by SDS-PAGE. Following SDS-PAGE, Western blot analysis using a DNP-specific antibody was carried out (upper panel). Equal amounts of purified Cu,Zn-SOD (0.8 μg) were immunostained with anti-Cu,Zn-SOD antibody as internal standard (lower panel). Lane 1 represent incubation without H_2O_2 (control); lane 2, 0.5 mM H_2O_2; lane 3, 1.0 mM H_2O_2.

H_2O_2 increased with increasing concentrations of H_2O_2 (Figure 5, upper panel, lane 2 and 3).

Overall patterns of changes in protein expression

Figure 6 shows the protein spots in 2D-gels from liver tissue of SAMP8 at 9 month. Image analysis of the gels detected about 200 spots using CBB R-350 staining. We focused on proteins which showed the density at least >1.5-fold between strains. The proteins which were down regulated in SAMP8 compared with SAMR1 were 7 spots, of which 2 spots were identified (spot 1, 78 kDa glucose-regurated protein (GRP78/Bip); spot 6, methionine adenosyltransferase (MAT)). The proteins which were up-regulated in SAMP8 compared with SAMR1 were 3 spots, of which only one spot was identified (spot 9, MUP). Other proteins (spot 2, serum albumin; spot 4, PDI ER-60; spot 5, SBP; spot 11, Cu,Zn-SOD) were demonstrated no significant change of expression level between SAMP8 and SAMR1.

The protein name, MW/pI, MOWSE score, MS-digest index number, accession number, database for identification and change in expression between strains are summarized in Table I. These identified protein spots are numbered as shown in Figure 6.

Discussion

This study firstly showed proteomics data by 2D-Oxyblot and identification of carbonylated proteins in SAM strains. Carbonylated antioxidant proteins, such as Cu,Zn-SOD, serum albumin and SBP increased in the young (3-month old) SAMP8 liver. Cu,Zn-SOD is one of key enzymes in protecting the cell from oxygen toxicity [14]. It has been reported that the mitochondrial Cu,Zn-SOD activities decreased in livers in SAMP strain compared with SAMR strain [15]. To elucidate the mechanism of carbonylation of Cu,Zn-SOD, we examined carbonyl modification of purified Cu,Zn-SOD induced by H_2O_2. Carbonyl modification of Cu,Zn-SOD increased with increasing concentrations of H_2O_2. When Cu,Zn-SOD is incubated with relatively high levels of H_2O_2, it may become inactivated and then releases copper which can, with the H_2O_2, constitute a Fenton system. H_2O_2 reacts with copper leading to form bound hydroxyl radical such as Cu(I)-hydroperoxo complex, which may release ·OH [16]. It is considered that carbonyl

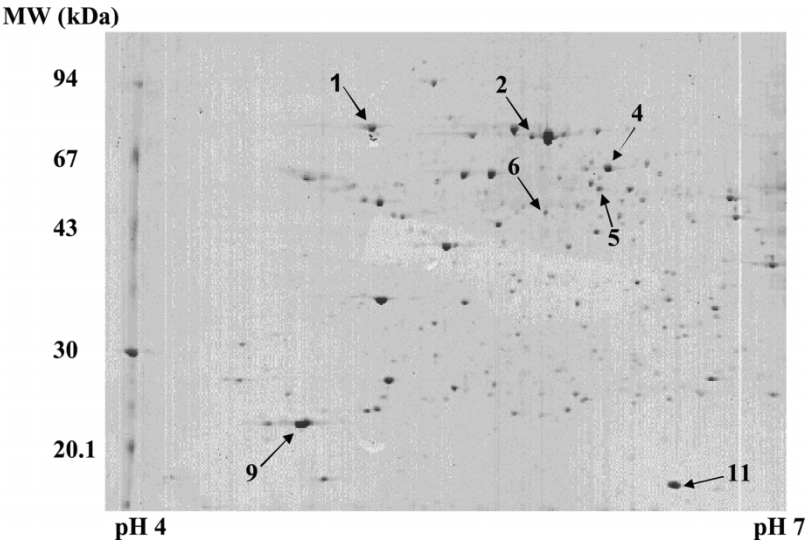

Figure 6. The protein spots in 2D-gel from liver tissue of SAMP8. Spot 1 (1.5-fold) and 6 (2.0-fold), which were down regulated in SAMP8 compared with SAMR1, were identified as GRP78/Bip and MAT, respectively. Spot 9 (1.8-fold), which was up regulated in SAMP8 compared with SAMR1, was identified as MUP. Spots 2, 4, 5, and 11 which were no change between strains were identified as serum albumin, PDI ER-60 precursor, mouse SBP, and Cu,Zn-SOD, respectively.

Table I. Identification of aging-associated proteins as determined by MALDI-TOF MS.

No.*	Protein name	MW (Da)-pI	MOWSE score	MS-digest index#	Accession#	Database	Change pattern	2D-Oxyblot no. (in Figures 2–3)
1	78 kDa Glucose-regurated protein (GRP78/Bip)	72423/5.1	7.450e + 05	105245	P20029	SwissProt	Down†	c4
2	Serum albumin	68693/5.7	4.999e + 05	78793	P07724	SwissProt	NC‡	c6
4	Protein disulfide isomerase ER-60 precursor (PDI)	56622/6.0	1.671e + 04	16345	ER60-MOUSE	Owl	NC	c7
5	Mouse selenium binding liver protein (SBP)	52352/6.0	3.870e + 04	49434	SBP-MOUSE	Owl	NC	c9
6	Metionine adenosyl transferase (MAT)	43537/5.5	3.480e + 04	773290	476917	NCBInr	Down	
9	Major urinary protein (MUP)	20649/5.0	3.350e + 06	37632	P11588	SwissProt	Up¶	c12
11	Superoxide dismutase[Cu-Zn] (Cu,Zn-SOD)	15943/6.0	1.455e + 04	8581	P08228	SwissProt	NC	c14
	Hippocampal neurostimulating peptide precursor protein (HCNP-pp)	20831/5.2	8.619e + 04	95447	P70296	SwissProt	NC	B2

* Spot numbers correspond to the numbered CBB staining 2D-gel image in liver (Figure 6).
† Down-regulated in SAMP8 (< − 1.5-fold). ‡ No change between SAMP8 and SAMR1. ¶ Up-regulated in SAMP8 (> 1.5-fold).

modification of Cu,Zn-SOD in SAMP8 may be caused by reactive oxygen species generated from H_2O_2 and metals. Relevantly, it is reported that H_2O_2 caused oxidative cleavage to Cu,Zn-SOD [17,18]. Accumulation of oxidative damage to antioxidant proteins, especially Cu,Zn-SOD may cause dysfunction of defense systems against oxidative stress in SAMP8 with a higher oxidative states, leading to acceleration of senescence.

We also demonstrated increase of carbonylated GRP78/Bip and PDI, which are specific ER resident proteins, in the SAMP8 liver compared with SAMR1. GRP78/Bip acts as a molecular chaperone in ER by associating transiently with incipient proteins and aiding in their folding and transport [19–21]. Increase of GRP78/Bip is induced by the ER stress response [21]. PDI is the archetypal catalyst of disulphide bound formation [22]. The primary function of disulphide bounds is to stabilize the folded structure of the protein, which in turn is essential for the correct function of the protein [22]. It has been reported that the age-associated increase in carbonyl modification of GRP78/BiP and PDI in mouse liver, could result in ER dysfunction [23]. Approximately one-third of all proteins are translocated into the ER where they undergo post-translational modifications, folding, disulfide bond formation, glycosylation and oligomerization assisted by ER chaperone, such as GRP78/Bip and PDI [24]. Our results and these literatures have suggested that protein folding, disulfide bond formation and glycosylation is more severely disrupted in SAMP8 compared with SAMR1. Several age-associated diseases, such as Alzheimer's disease (AD), are caused by conformational changes coupled to the aggregation of mis-folded proteins [25–27]. Elevation in oxidative damage to critical ER chaperones in the liver of SAMP8 may contribute to acceleration of aging. Therefore, increases of carbonyl modification of antioxidant proteins and ER chaperones can reasonably explain accelerating senescence in SAMP8.

We demonstrated increase in carbonylation of HCNP-pp in the SAMP8 brain compared with SAMR1 at 9 month. HCNP-pp is a unique multifunctional protein, being not only the precursor of HCNP but also the binding proteins of phosphatidylethanolamine, ATP, Raf-1 kinase and serine protease [28]. HCNP has been shown to involve in the development of specific cholinergic neurons in central nervous system [29,30]. The septohippocampal cholinergic system is implicated in learning and memory and dysfunction of the cholinergic system is involved in the dementia of AD [31]. In fact, a loss of cholinergic neurons innervating the hippocampus is observed in the brain tissues of AD patients [32]. Collectively, accumulation of oxidative damage to HCNP-pp may contribute to the age-accelerated deterioration in learning and memory in SAMP8.

We analyzed protein expression in aged (9-month old) SAMP8 liver using 2D-electrophoresis. Down-regulation of expression in MAT (2.0-fold) in SAMP8 compared with SAMR1 was observed. MAT catalyzes the production of S-adenosylmethionine (SAMe), which has antioxidant properties. [33,34]. We showed that up-regulation (about 2.0-fold) of MUP in the SAMP8 compared with SAMR1. MUP is present in high levels in the urine of mice [35] and MUP gene expression increases with aging [36]. Combination of these proteins can be expected to be candidates as valuable biomarkers of senescence acceleration.

Acknowledgements

We thank Dr. Hisaaki Taniguchi of The University of Tokushima for his support in LC-MS/MS analysis. This work was supported by Grants-in-Aid for Scientific Research from the Ministry of Education, Science, Sports and Culture of Japan.

References

[1] Takeda T, Hosokawa M, Takeshita S, Irino M, Matsushita T, Tomita Y, Yamashira K, Hamamoto H, Shimizu K, Ishii M, Yamamuro T. A new murine model of accelerated senescence. Mech Ageing 1981;17:83–194.

[2] Hosokawa M, Ueno M. Aging of blood–brain barrier and neuronal cells of eye and ear in SAM mice. Neurobiol Aging 1999;20:117–123.

[3] Butterfield DA, Howard JB, Yatin S, Allen LK, Carney MJ. Free radical oxidation of brain proteins in accelerated senescence and its modulation by *N*-tertbutyl-a-phenylnitrone. Proc Natl Acad Sci 1997;94:674–678.

[4] Kurokawa T, Asada S, Nishitani S, Hazeki O. Age-related changes in manganese superoxide dismutase activity in the cerebral cortex of senescence-accelerated prone and resistant mouse. Neurosci Lett 2001;298:135–138.

[5] Getchell VT, Peng X, Stromberg JA, Chan CK, Green CP, Subhedar KN, Shah SD, Mattson PM, Getchell LM. Age-related trends in gene expression in the chemosensorynasal mucosae of senescence-accelerated mice. Ageing Res Rev 2003;2:211–243.

[6] Hosokawa M. A higher oxidative status accelerates senescence and aggravates age-dependent disorders in SAMP strains of mice. Mech Ageing 2002;123:1553–1561.

[7] Yasui F, Ishibashi M, Matsugo S, Kojo S, Oomura Y, Sasaki K. Brain lipid hydroperoxide level increases in senescence-accelerated mice at an early age. Neurosci Lett 2003; 350:66–68.

[8] Takeda T, Hosokawa M, Higuchi K. Senescence-accelerated mouse (SAM): A novel murine model of accelerated senescence. J Am Geriatr Soc 1991;39:911–919.

[9] Cho MY, Bae HS, Choi KB, Cho YS, Song WC, Yoo KJ, Paik KY. Differential expression of the liver proteome in senescence accelerated mice. Proteomics 2003;3:1883–1894.

[10] Butterfield DA, Koppal T, Howard B, Subramaniam R, Hensley K, Yatin S, Allen K, Aksenov M, Aksenov M, Caeney J. Structural and functional changes in proteins induced by free radical-mediated oxidative stress and protective action of the antioxidants *N-tert*-butyl-alpha-phenylnitrone and vitamin E. Ann NY Acad Sci 1998;854:448–462.

[11] Berlett SB, Stadtman RE. Protein oxidation in aging, disease, and oxidative stress. J Biol Chem 1997;272:20313–20316.

[12] Castegna A, Aksenov M, Aksenova M, Thongboonkerd V, Klein BJ, Pierce MW, Booze R, Markesbery RW, Butterfield DA. Proteomic identification of oxidatively modified proteins in Alzheimer's disease brain. Part 1: Creatine kinase BB, glutamine synthase, and ubiquitin carboxyl-terminal hydrolase L-1. Free Radic Biol Med 2002;33:562–574.

[13] Levine RL, Garland D, Oliver CN, Amici A, Climent I, Lenz AG, Ahn BW, Shaltiel S, Stadtman ER. Determination of carbonyl content in oxidatively modified proteins. Methods Enzymol 1990;186:464–478.

[14] Kang HJ, Kim MS. DNA cleavage by hydroxyl radicals generated in the Cu,Zn-superoxide dismutase and hydrogen peroxide system. Mol Cells 1997;7:777–782.

[15] Park JW, Choi CH, Kim MS, Chung MH. Oxidative status on senescenceaccelerated mice. J Gerontol A Biol Sci 1996;51:B337–B345.

[16] Kawanishi S, Hiraku Y, Oikawa S. Mechanism of guanine-specific DNA damage by oxidative stress and its role in carcinogenesis and aging. Mutat Res 2001;488:65–76.

[17] Ookawara T, Kawamura N, Kitagawa Y, Taniguchi N. Site-specific and random fragmentation of Cu,Zn-superoxide dismutase by glycation reaction. Implication of reactive oxygen species. J Biol Chem 1992;267:18505–18510.

[18] Sato K, Akaike T, Kohno M, Ando M, Maeda H. Hydroxyl radical production by H_2O_2 plus Cu,Zn-superoxide dismutase reflects the activity of free copper released from the oxidatively damaged enzyme. J Biol Chem 1992;267:25371–25377.

[19] Kaufman JR. Stress signaling from the lumen of the endoplasmic reticulum: Coordination of gene transcriptional and translational controls. Genes 1999;13:1211–1233.

[20] Yoshida H, Haze K, Yanagi K, Yura T, Mori K. Identification of the *cis*-acting endoplasmic reticulum stress response element resposible for transcriptinal induction of mammalian glucouse-regulated proteins. J Biol Chem 1998;273: 33741–33749.

[21] Roy B, Lee SA. The mammalian endoplasmic reticulum stress response element consists of an evolutionarily conserved tripartite structure and interacts with a novel stress-inducible complex. Nucleic Acids Res 1999;27:1437–1443.

[22] Lappi KA, Lensink FM, Alanen IH, Salo HEK, Lobell M, Juffer HA, Ruddock WL. A conserved arginine plays a role in the catalytic cycle of the protein disulfide Isomerases. J Mol Biol 2004;335:283–295.

[23] Chang PW, Tsui SK, Liew C, Lee CC, Waye MM, Fung KP. Isolation, characterization, and chromosomal mapping of a novel cDNA clone encoding human selenium binding protein. J Cell Biochem 1997;64:217–224.

[24] Rabek PJ, Boylston III HK, Papaconstantinou J. Carbonylation of ER chaperone proteins in aged mouse liver. Biochem Biophys Res Commun 2003;305:566–572.

[25] Stefani M, Dobson MC. Protein aggregation and aggregate toxity: New insights into protein folding, misfolding diseases and biological evolution. J Mol Med 2003;81:678–699.

[26] Rakhit R, Cunningham P, Furtos-Matei A, Dahan S, Qi FX, Crow PJ, Casham RN, Kondejewski HL, Chakrabartty A. Oxidation-induced misfolding and aggregation of superoxide dismutase and its implications for amyotrophic leteral sclerosis. J Biol Chem 2002;277:47551–47556.

[27] Cohen EF, Kelly WJ. Therapeutic approaches to protein-misfolding diseases. Nature 2003;426:905–909.

[28] Ojika K, Mitake S, Tohdoh N, Appel HS, Otsuka Y, Katada E, Matsukawa N. Hippocampal cholinergic neurostimulating peptides (HCNP). Prog Neurobiol 2000;60:37–83.

[29] Levey IA. Muscarinic acetylcholine receptor expression in memory circuits: Implications for treatment of Alzheimer disease. Proc Natl Acad Sci 1996;93:13541–13546.
[30] Ojika K, Mitake S, Kayama T, Taiji M. Two different molecules, NGF and free-HCNP, stimulate cholinergic activity in septal nuculei *in vitro* in a different manner. Brain Res Dev Brain Res 1994;79:1–9.
[31] Ojika K, Appel HS. Neurotrophic effects of hippocampal extracts on medial septal nucleus *in vitro.* Proc Natl Acad Sci 1984;81:2567–2571.
[32] Whitehouse PJ, Price DL, Struble RG, Clark AW, Coyle JT, Delon MR. Alzheimer's disease and senile dementia: Loss of neurons in the basal forebrain. Science 1982;215:1237–1239.
[33] Avila AM, Corrales JF, Ruiz F, Sánchez-Góngra E, Mingorance J, Carretero VM, Mato MJ. Specific interaction of methionine adenosyltransferase with free radicals. Biofactor 1998;8:27–32.
[34] Trolin GC, Löfberg C, Trolin G, Orelamd L, Brain. ATP:L-methionine S-adenosyltransferase (MAT) S-adenosylmethionine (SAM) and S-adenosylhomocysteine (SAH): Regional distribution and age-related changes. Eur Neuropsychopharmacol 1994;4:469–477.
[35] Beynon RJ, Veggerby C, Payne CE, Robertson DL, Gaskell SJ, Humphries RE, Hurst JL. Polymorphism in major urinary proteins: Molecular heterogeneity in a wild mouse population. J Chem Ecol 2002;28:1429–1446.
[36] Friedman V, Wagner J, Danner DB. Isolation and identification of aging-related cDNAs in the mouse. Mech Ageing Dev 1990;52:27–43.